Assessment of Sea Ice Classification Capabilities During Melting Period Using Airborne Multi-frequency PolSAR Data

Peng Wang [1,2], Xi Zhang [1,2,*], Lijian Shi [3], Meijie Liu [4], Genwang Liu [2], Chenghui Cao [2] and Ruifu Wang [1]

[1] College of Geodesy and Geomatics, Shandong University of Science and Technology, China;
[2] First Institute of Oceanography, Ministry of Natural Resources, Qingdao 266061, China;
[3] National Satellite Ocean Application Service, Beijing 100081, China;
[4] Qingdao University, Qingdao 266071, China;

Abstract

Sea ice mapping using Synthetic Aperture Radar (SAR) in the melt season poses challenges, primarily due to meltwater complicating the distinguishability of sea ice types. In response to this issue, this study introduces a novel method for classifying sea ice during the Bohai Sea's melting period. The method categorizes sea ice into five types: Open Water (OW), Grey Ice (Gi), Melting Grey Ice (GiW), Grey-White Ice (Gw), and Melting Grey-White Ice (GwW). To achieve this classification, 51 polarimetric features are extracted from L, S, and C-band PolSAR data using various polarization decomposition methods. The study assesses the separability of these features among different sea ice type combinations by calculating the Euclidean distance (ED). The Support Vector Machine (SVM) classifier, when employed with single-frequency polarimetric feature sets, achieves the highest accuracy for OW and Gi in the C-band, GiW in the S-band, and Gw and GwW in the L-band. Remarkably, the C-band features exhibit the overall highest accuracy when compared to the L and S bands. Furthermore, employing a multi-dimensional polarimetric feature set significantly improves classification accuracy to 94.55%, representing a substantial enhancement of 9% to 22% compared to single-frequency classification. Benefiting from the performance advantages of Random Forest (RF) classifier in handling large data sets, RF classifiers achieve the highest classification accuracy of 95.84%. The optimal multi-dimensional feature composition includes: L-band: SE, SE_I, $\bar{\alpha}$, Span; S-band: SE_I, SE, Span, $P_{V\text{-}Freeman}$, λ_1, λ_2; C-band: SE, SE_I, Span, λ_3, $P_{V\text{-}Freeman}$. The results of this study provide a reliable new method for future sea ice monitoring during the melting season.

Study Area And Data

Study Area

The research area for this study is located in Liaodong Bay, situated within the Bohai Sea region of China, as illustrated in Figure 1.

- Longitude range: 121° 57'E to 122° 10'E
- Latitude range: 40° 8'N to 40° 22'N

Sea ice in the Bohai Sea is of the annual type, forming during the winter and persisting until early spring of the following year.

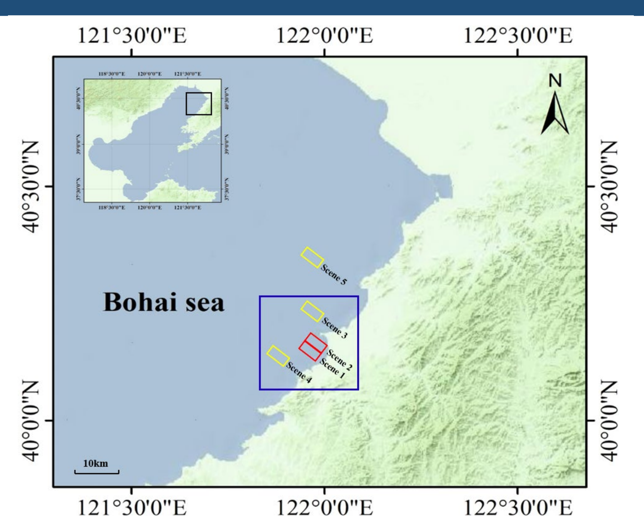

Figure 1. The map of study area in the vicinity of Bayuquan in Liaodong Bay.

Airborne Multi-frequency PolSAR data

- Time(UTC): 2022-02-27T06:22:54
- Frequency: L/S/C
- Resoultion: 1/1/0.5 m
- Flight altitude: 4710 m
- Incidence angle: 31°~34°
- Temperatures: 6~10℃
- Wind speed: 3~8 m/s

Sentinel-2 MSI data

- Time(UTC): 2022-02-27T02:36:39

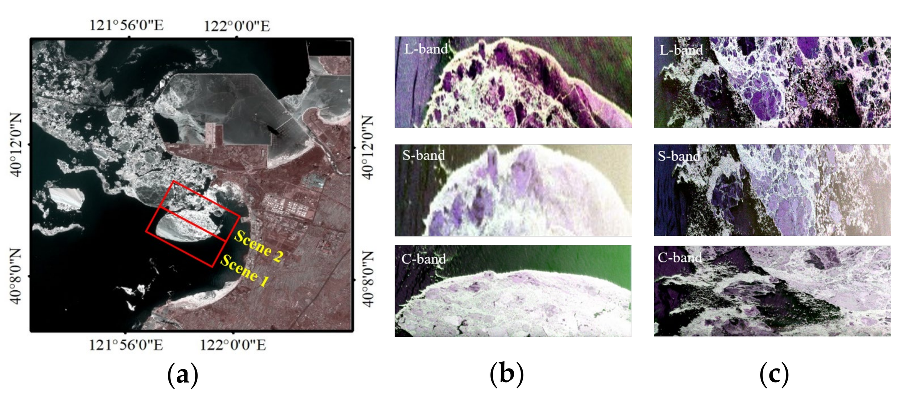

Figure 2. (a)The Sentinel-2 true-color image . The red rectangles in the image indicate the coverage area of the PolSAR data in Scene 1 and Scene 2. For each waveband, the partially overlapping regions in (b) Scene 1 and (c) Scene 2 are represented in Pauli RGB images.

Visual interpretation

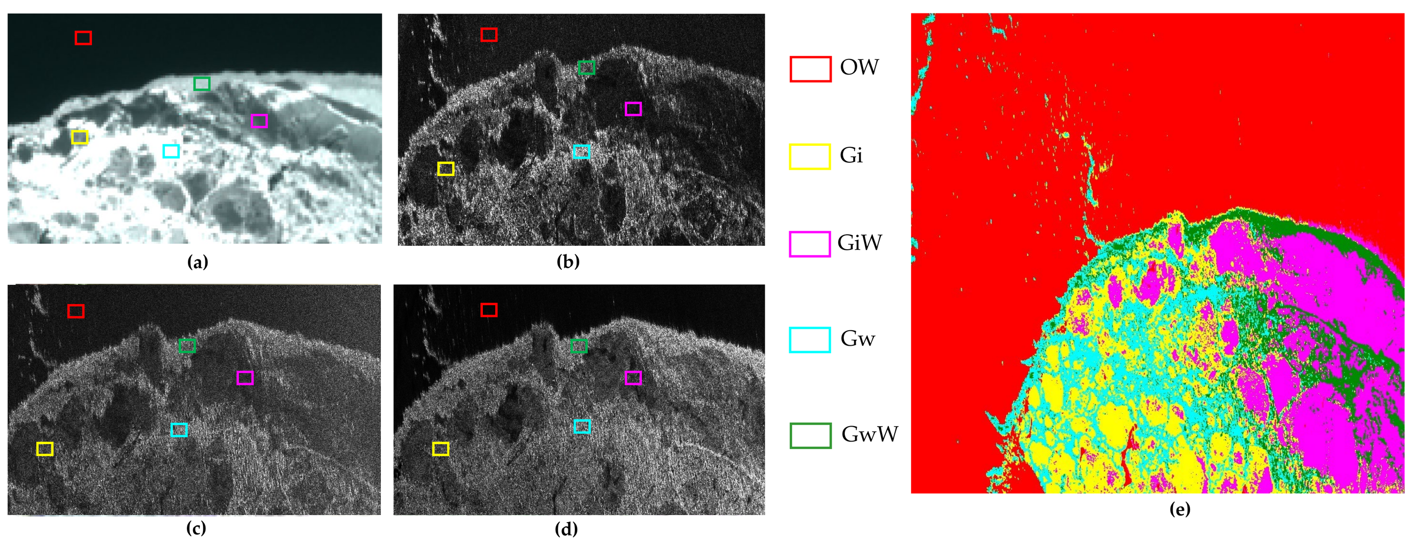

Figure 3. (a) Sample examples of different sea ice types in Sentinel-2 imagery, (b) L-band, (c) S-band, (d) C-band images in Scene 1; (e) expert interpretation map.

Methods

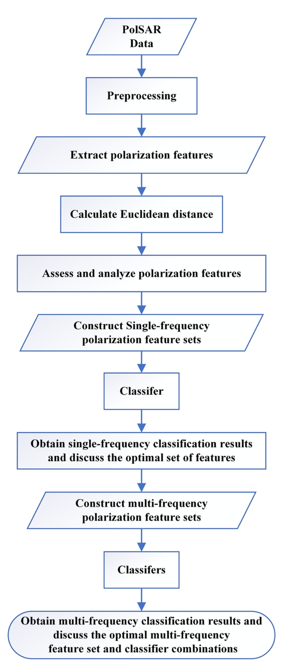

Figure 4. Flowchart of sea ice classification during melting period with multi-frequency PolSAR data.

Table 1. Polarimetric features in this study.

The target polarization decomposition based scattering model	Freeman-Durden decomposition	Surface Scattering(P_S), Double Bounce Scattering (P_D), Volume Scattering (P_V)
	Yamaguchi decomposition	Surface Scattering(P_S), Double Bounce Scattering (P_D), Volume Scattering (P_V), Helix Scattering（P_h）
H/A/$\bar{\alpha}$ decomposition		Eigenvalue($\lambda_1, \lambda_2, \lambda_3$), Eigenvector ($P_1, P_2, P_3$) , Polarization scattering entropy(H), Eigen component (β, δ, γ), Anisotropy(A, A_{12}), Shannon entropy(SE, SE_P, SE_I), Single bounce eigenvalues relative difference($SERD$), Double bounce eigenvalues relative difference($DERD$), Polarization fraction (PF), Polarimetric asymmetry (PA), Radar vegetation index (RVI), Pedestal height (PH), Alpha approximation ($\bar{\alpha}$), Consistency correlation coefficient(CCC), Covariance matrix diagonal elements (C_{11}, C_{22}, C_{33})
Other parameters		Span of coherency matrix T3($Span$)、Polarization correlation coefficient($\rho_{12}, \rho_{13}, \rho_{23}$)

The sea ice type discrimination ability of 51 polarization features in 3 bands was evaluated

Separability Index

- Euclidean distance

$$D = \frac{|m_1 - m_2|}{\sqrt{\sigma_1^2 + \sigma_2^2}}$$

- Ice Type

$$Ice\ Type = \sum_{i=10} D_i$$

- Average Euclidean distance(A_{ED})

$$A_{ED} = \frac{\sum D_j}{N}$$

Evaluation indicators

$A_{ED} \geq 1.2$ → **High** separability

$1.2 \geq A_{ED} \geq 0.6$ → **Medium** separability

$0.6 \geq A_{ED}$ → **Low** separability

Classifier

- Maximum Likelihood classification (ML)
- Support Vector Machines (SVM)
- Random Forest (RF)
- Back propagation neural network (BPNN)

Result

Single-frequency Polarimetric Features Analysis

- L-band

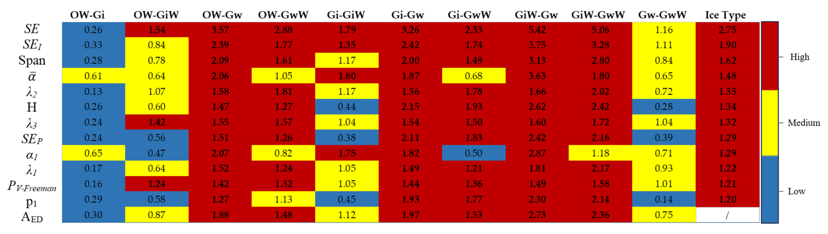

Figure 5. The Euclidean distance of L-band polarimetric features in different type combinations.

- ✓ Shannon entropy has the highest ice type discrimination ability.
- ✓ Good discrimination ability among sea ice types.
- ✓ Poor discrimination in OW-Gi separation and Gw-GwW separation.

- S-band

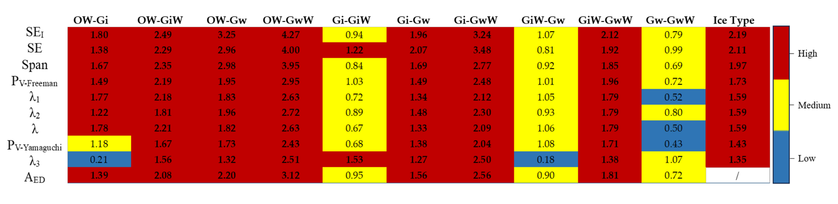

Figure 6. The Euclidean distance of S-band polarimetric features in different type combinations.

- ✓ Intensity component of shannon entropy has the highest ice type discrimination ability.
- ✓ Good discrimination ability between OW and sea ice.
- ✓ Poor discrimination in GiW-Gw separation and Gw-GwW separation.

- C-band

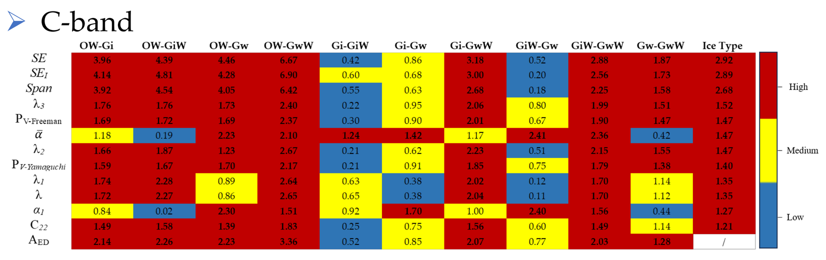

Figure 7. The Euclidean distance of S-band polarimetric features in different type combinations.

- ✓ Shannon entropy has the highest ice type discrimination ability.
- ✓ Good discrimination ability between OW and sea ice.
- ✓ Poor discrimination in Gi-GiW separation and Gi-Gw separation.

Sea Ice Classification

- Single-frequency Sea Ice Classification

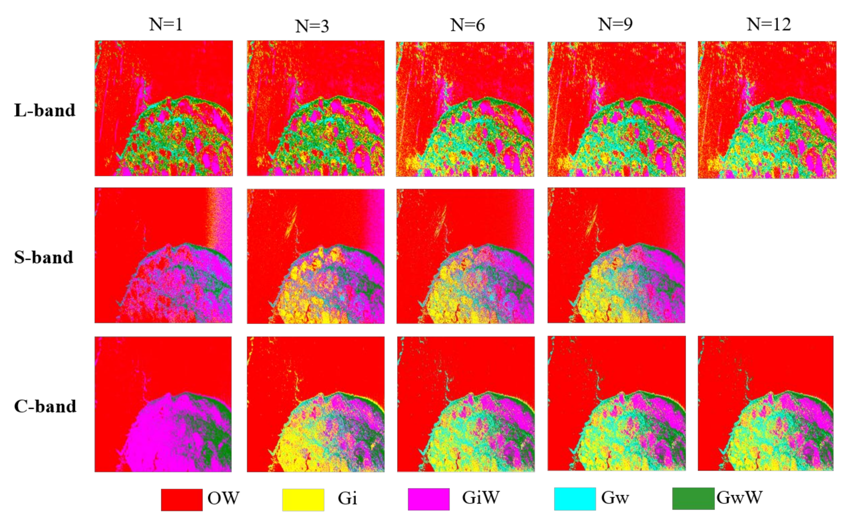

Figure 8. The partial classification result images for Scene 1 by using SVM. Each row represents a different band, and each column represents the corresponding number of polarization features.

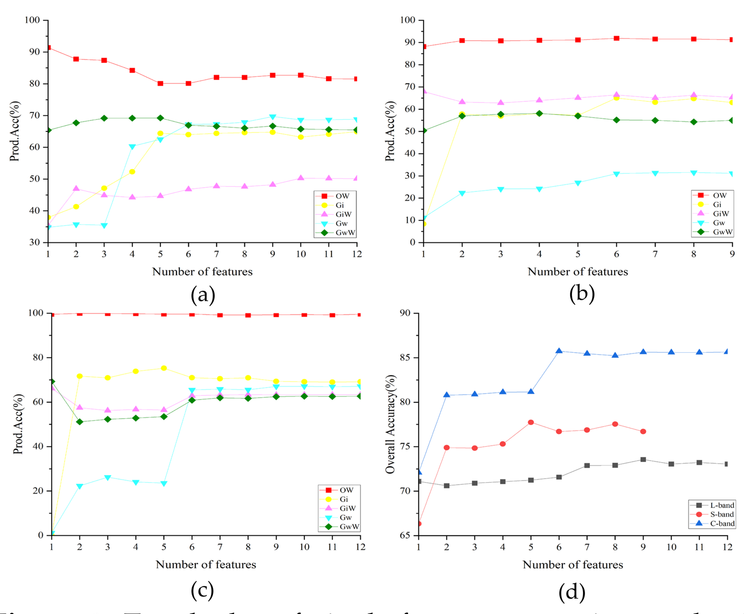

Figure 9. Trend plot of single-frequency sea ice production accuracy for Scene 1.

- ✓ The L-band has highest classification accuracy for Gw and GwW;
- ✓ The S-band has highest classification accuracy for Gi and GiW;
- ✓ The C-band has highest classification accuracy for OW.

- Multi-frequency Sea Ice Classification

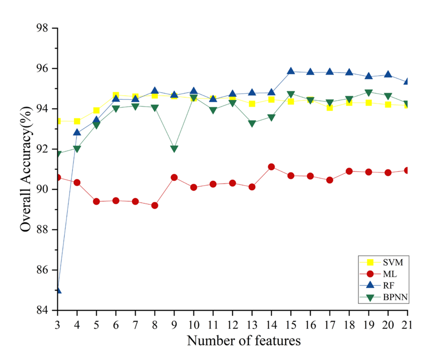

Figure 10. The overall accuracy trends for different classifiers in Scene 1.

Table 2. Each classifier corresponds to the composition of the optimal multi-dimensional polarization feature set.

Classifier	Polarimetric Features	Total
SVM	C-SE, C-SE_I, L-SE, C-span, S-SE_I, S-SE, S-span, L-SE_I, S-$P_{V\text{-}Freeman}$, L-span, S-λ_1, S-λ_2	12
ML	C-SE, C-SE_I, L-SE, C-span, S-SE_I, S-SE, S-span, L-SE_I, S-$P_{V\text{-}Freeman}$, L-span, S-λ_1, S-λ_2, C-λ_3, L-$\bar{\alpha}$	14
RF	C-SE, C-SE_I, L-SE, C-span, S-SE_I, S-SE, S-span, L-SE_I, S-$P_{V\text{-}Freeman}$, L-span, S-λ_1, S-λ_2, C-λ_3, L-$\bar{\alpha}$, C-$P_{V\text{-}Freeman}$	15
BPNN	C-SE, C-SE_I, L-SE, C-span, S-SE_I, S-SE, S-span, L-SE_I, S-$P_{V\text{-}Freeman}$, L-span, S-λ_1, S-λ_2, C-λ_3, L-$\bar{\alpha}$, C-$P_{V\text{-}Freeman}$, C-$\bar{\alpha}$, C-λ_2, S-$P_{V\text{-}Yamaguchi}$, L-λ_3	19

- ✓ The RF classifier's classification accuracy continues to improve and achieves the highest overall accuracy in this experiment. This advantage may be attributed to its suitability for handling large datasets compared to other classifiers.

Validation and Comparison

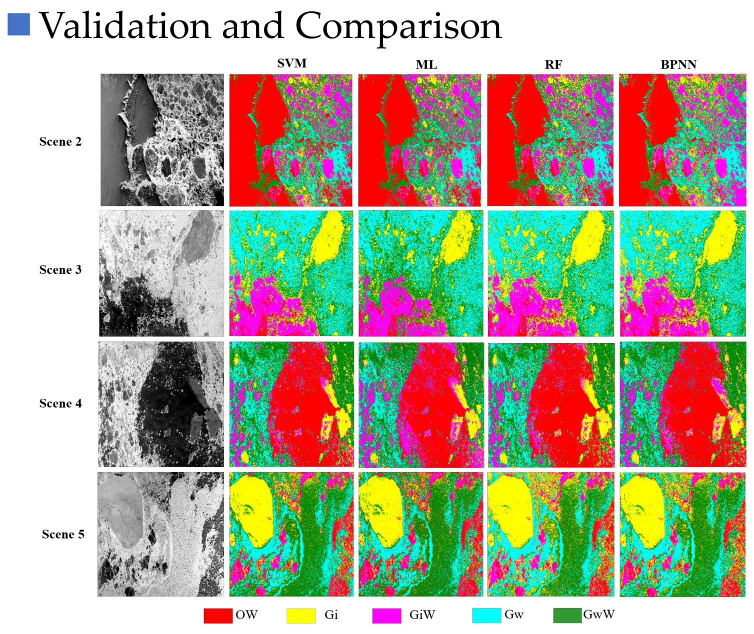

Figure 11. Validation data and classification results

Table 3. Dual polarization data and previous research classification accuracy table

Band	Polarization Mode	Scene	Overall Accuracy
L	HH+HV	Scene 1	58.57%
	HH+HV	Scene 5	63.68%
C	HH+HV	Scene 1	64.52%
	HH+HV	Scene 5	55.23%
	HH+HV+VH+VV	Scene 1	79.31%
	HH+HV+VH+VV	Scene 5	68.89%

- ✓ The accuracy is higher with multi-band full-polarization data in different scenarios. This confirms the superiority of full-polarization data over using only dual-polarization data.
- ✓ The comparison with previous studies on C-band data further validates the feasibility of using multi-band data for sea ice classification during the melting period.

Conclusion

In the case of using the SVM classifier, the multidimensional polarization feature set exhibited improved classification accuracy compared to the three single-frequency polarization feature sets, with improvements ranging from 9% to 22%. The highest classification accuracy among different feature-classifier combinations was achieved when using the RF classifier at 95.84%. We validated our proposed method using verification data, and the results similarly demonstrated that our method is effective for classifying sea ice types OW, Gi, GiW, Gw, and GwW during the melting season in the Bohai Sea.